

## Electronic supplementary information

### Secondary ligand-induced orthogonal self-assembly of silver nanoclusters into superstructures with enhanced NIR emission

Korath Shivan Sugi,<sup>a</sup> Amritha P Sandra,<sup>a</sup> Nonappa,<sup>b</sup> Debasmita Ghosh,<sup>a</sup> Jyoti Sarita Mohanty,<sup>a</sup> Murugesan Paulthangam Kannan,<sup>a</sup> B. S. Sooraj,<sup>a</sup> Pillalamarri Srikrishnarka,<sup>a</sup> Jayoti Roy,<sup>a</sup> Wakeel Ahmed Dar,<sup>a</sup> and Thalappil Pradeep<sup>\*a</sup>

<sup>a</sup> DST Unit of Nanoscience (DST UNS) and Thematic Unit of Excellence (TUE), Department of Chemistry, Indian Institute of Technology Madras, Chennai 600 036; India; International Centre for Clean Water, Chennai 600113, India

<sup>b</sup> Faculty of Engineering and Natural Sciences, Tampere University, FI-33720 Tampere, Finland

\*E-mail: pradeep@iitm.ac.in

#### Table of contents

SL. No.	Description	Page No.
	Serial EM and electron tomography reconstruction	2
	ESI MS conditions	2
Fig. S1	Collision-induced dissociation mass spectra of the Ag <sub>14</sub> nanoclusters	3
Fig. S2	SEM image and EDS mapping of Ag <sub>14</sub> nanoclusters	4
Fig. S3	XPS of Ag <sub>14</sub> nanoclusters	4
Fig. S4	<sup>31</sup> P NMR of Ag <sub>14</sub> nanoclusters	5
Fig. S5	TEM images showing the structural evolution of Ag <sub>14</sub> nanoclusters with the addition of different molar ratios of DPPH ligand	6
Fig. S6	Large area TEM images of NCA-1.0	7
Fig. S7	Large area HRTEM images of NCA 1.0	8

Fig. S8	STEM images of NCA-1.0	9
Fig. S9	STEM-EDS mapping of NCA-1.0	9
Fig. S10	STEM-EDS mapping of spherical structures in NCA-1.0	10
Fig. S11	EDX spectrum of NCA-1.0	10
Fig. S12	The $^{31}\text{P}$ NMR spectra of NCA 0.5 and NCA 1.0.	11
Fig. S13	The $^{31}\text{P}$ NMR spectra of NCA 3.0, NCA 5.0, and NCA 10.0.	11
Fig. S14	UV-vis spectrum and ESI MS of NCA-1.0 redispersed in DMF	12
Fig. S15	TEM images of the DPPH-NT mixture	12
Fig. S16	Schematic illustration of supramolecular interactions in $\text{Ag}_{14}$ nanoclusters	13

**Serial EM and electron tomography reconstruction:** The image acquisition was performed using a JEOL JEM-3200FSC field emission TEM operated at 300 kV with an Omega-type zero-loss filter. The tilt series of 2D projections (between  $\pm 69^\circ$  angles with  $2^\circ$  increment steps) were recorded using SerialEM software.<sup>1-3</sup> The pre-alignment and final alignment were performed using IMOD software.<sup>4</sup> Finally, the maximum entropy method (MEM),<sup>5</sup> was used with a custom-made program with a regularization parameter value of  $\lambda = 1.0\text{e}^{-3}$  for reconstruction and colored tomograms were prepared using Chimera software.

### ESI MS conditions

Sample concentration: 10  $\mu\text{g}/\text{mL}$

Solvent: DCM/TCM/DMF

Flow rate: 30  $\mu\text{L}/\text{min}$

Capillary voltage: 2 kV

Source temperature: 50°C

Sampling cone: 0

Source offset: 0

Desolvation temperature: 65°C

Desolvation gas flow: 400.0 L/h

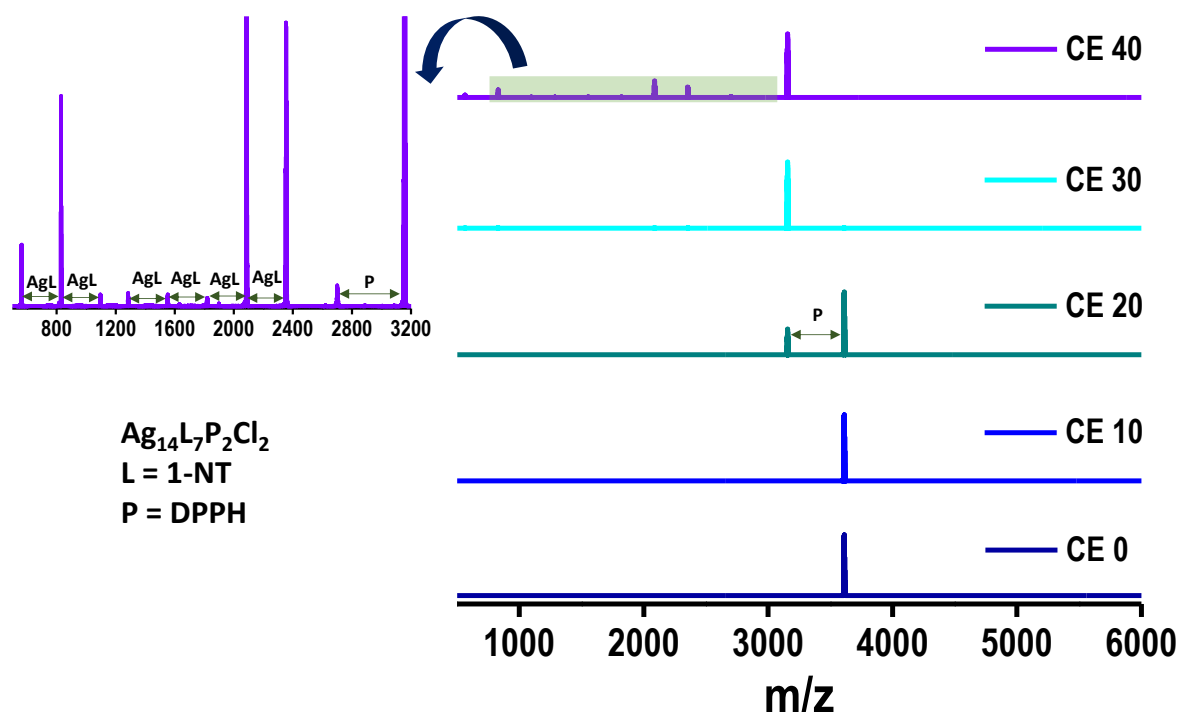


**Fig. S1 A)** Collision-induced dissociation (CID) mass spectra of the peak which is assigned as  $[\text{Ag}_{14}(\text{NT})_7(\text{DPPH})_2\text{Cl}_2]^+$ . The systematic loss of two DPPH ligands upon the increase in collision energy was observed along with the loss of some Ag-L.

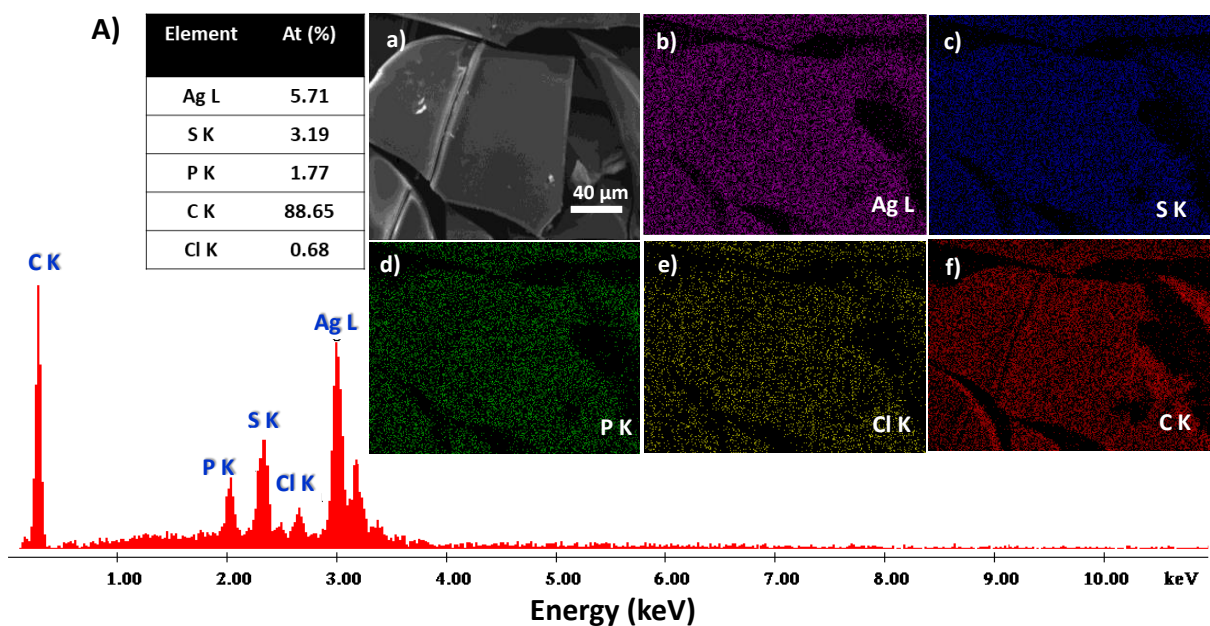


**Fig. S2** A) SEM image and EDS mapping of b) Ag L, c) S K, d) P K, e) Cl K, and f) C K.

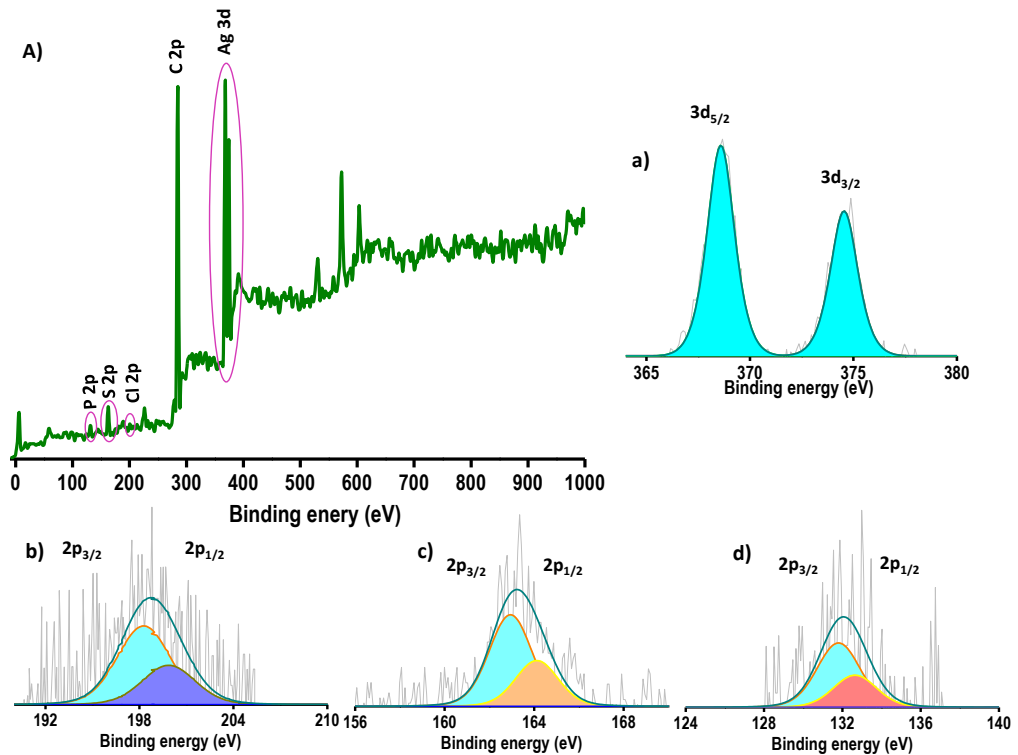


**Fig. S3** A) XPS survey spectrum of  $[\text{Ag}_{14}(\text{NT})_7(\text{DPPH})_2\text{Cl}_2]^+$ . Expanded area of a) Ag 3d, b) Cl 2p, c) S 2p, and d) P 2p.

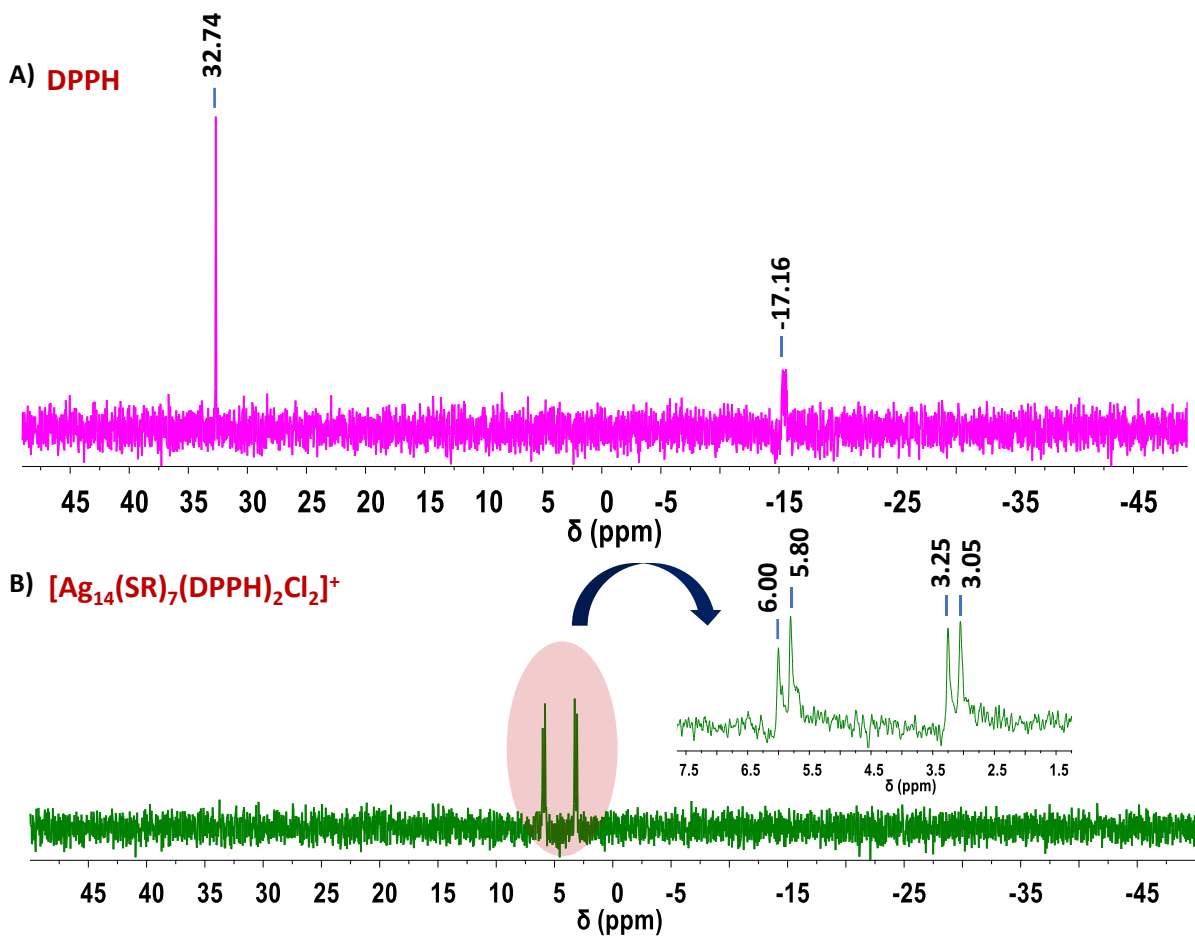


**Fig. S4** The  $^{31}\text{P}$  NMR spectra of A) DPPH and B)  $[\text{Ag}_{14}(\text{NT})_7(\text{DPPH})_2\text{Cl}_2]^+$  NCs confirm the formation of Ag-P bonds.

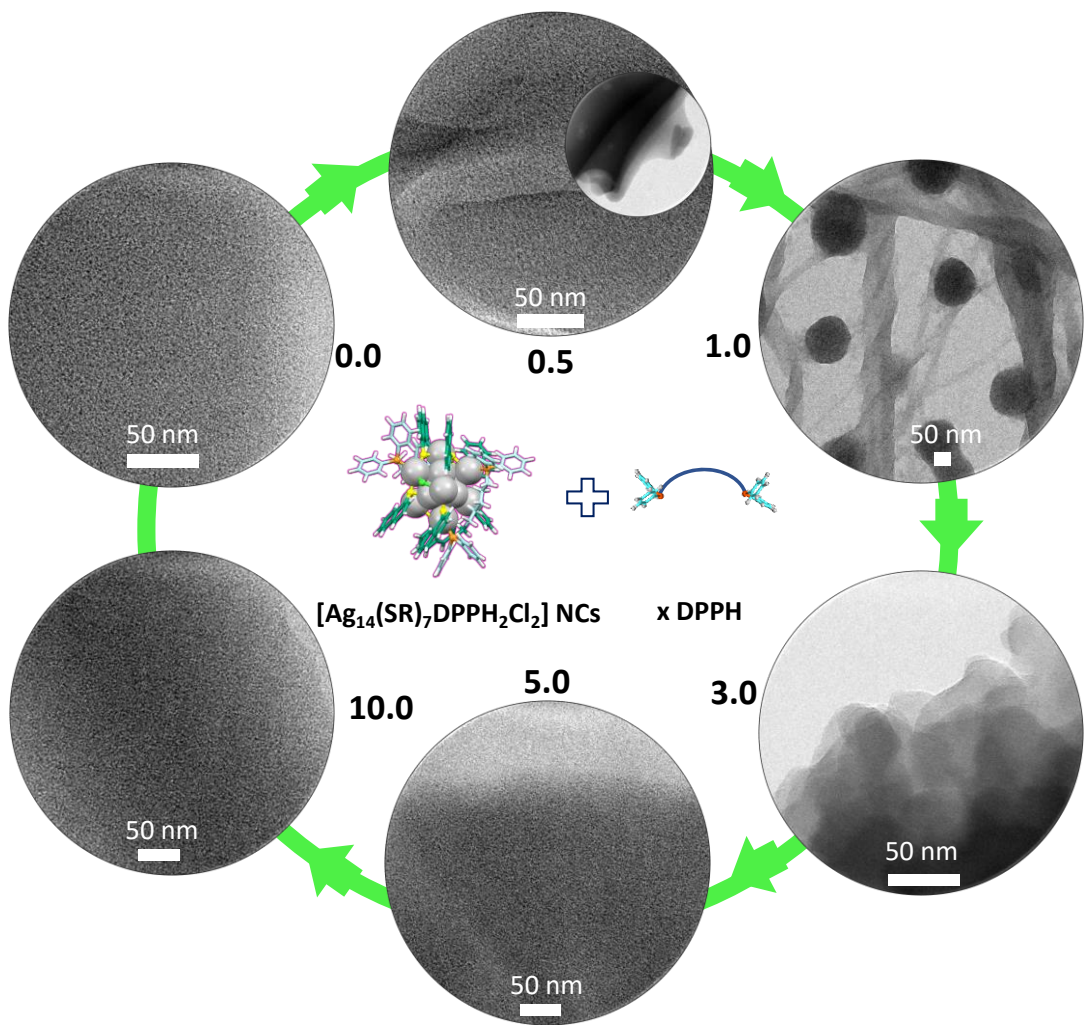


**Fig. S5** TEM images showing the structural evolution of  $[\text{Ag}_{14}(\text{NT})_7(\text{DPPH})_2\text{Cl}_2]^+$  NCs with the addition of different molar ratios of DPPH ligand.

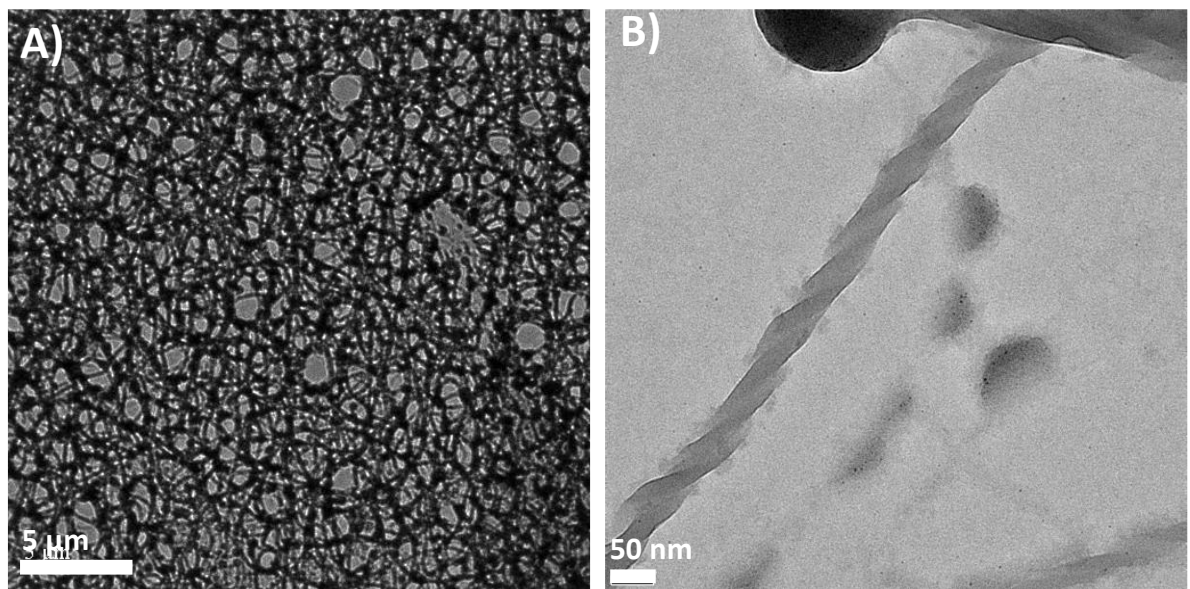


**Fig. S6** A) Large area TEM images of NCA-1.0. B) Expanded view of super helical structures.

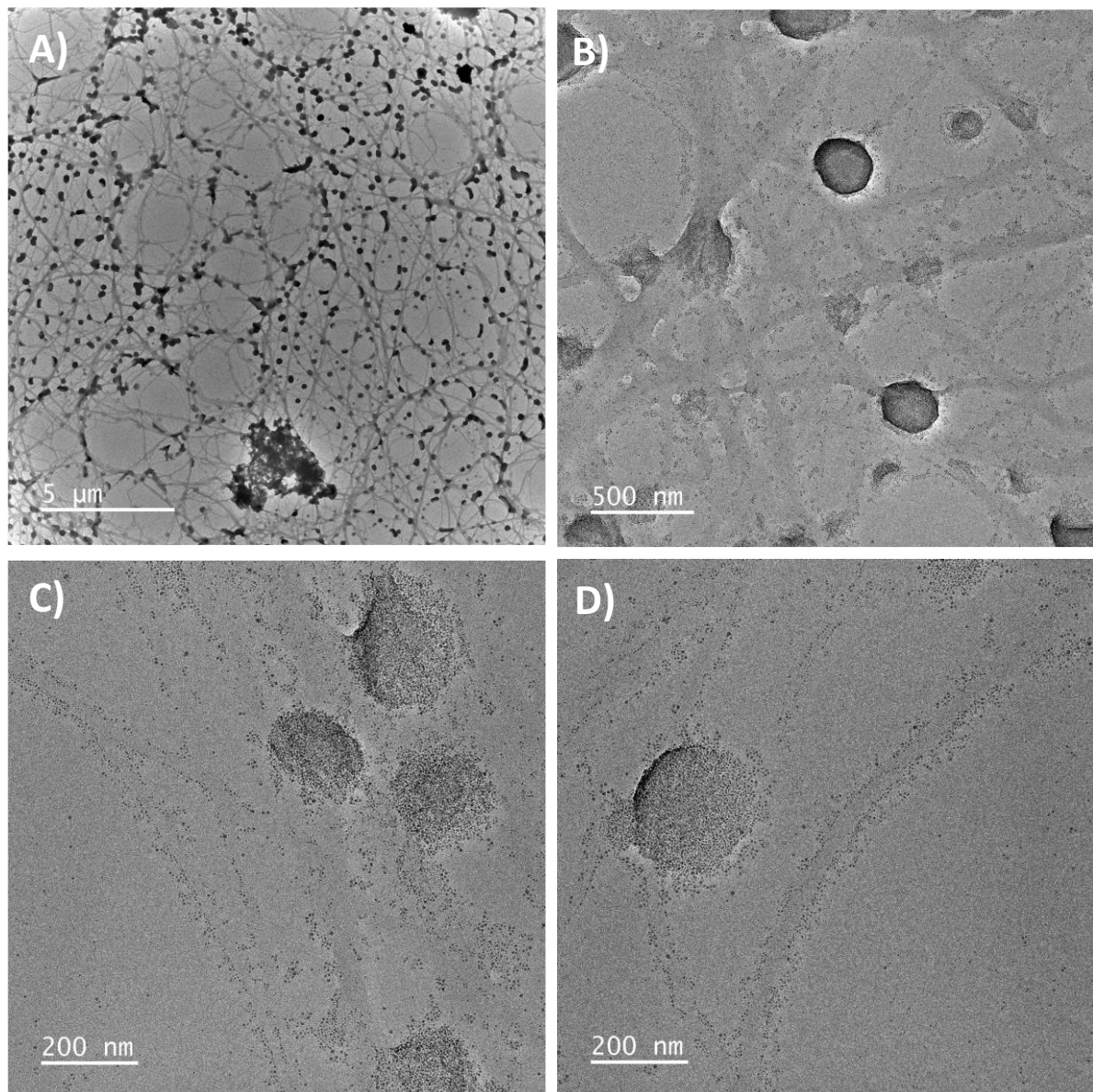


**Fig. S7** A) Large area HRTEM images of NCA-1.0. B), C), and D) are the expanded view which confirms the presence of nanoclusters in the helical and spherical structures.

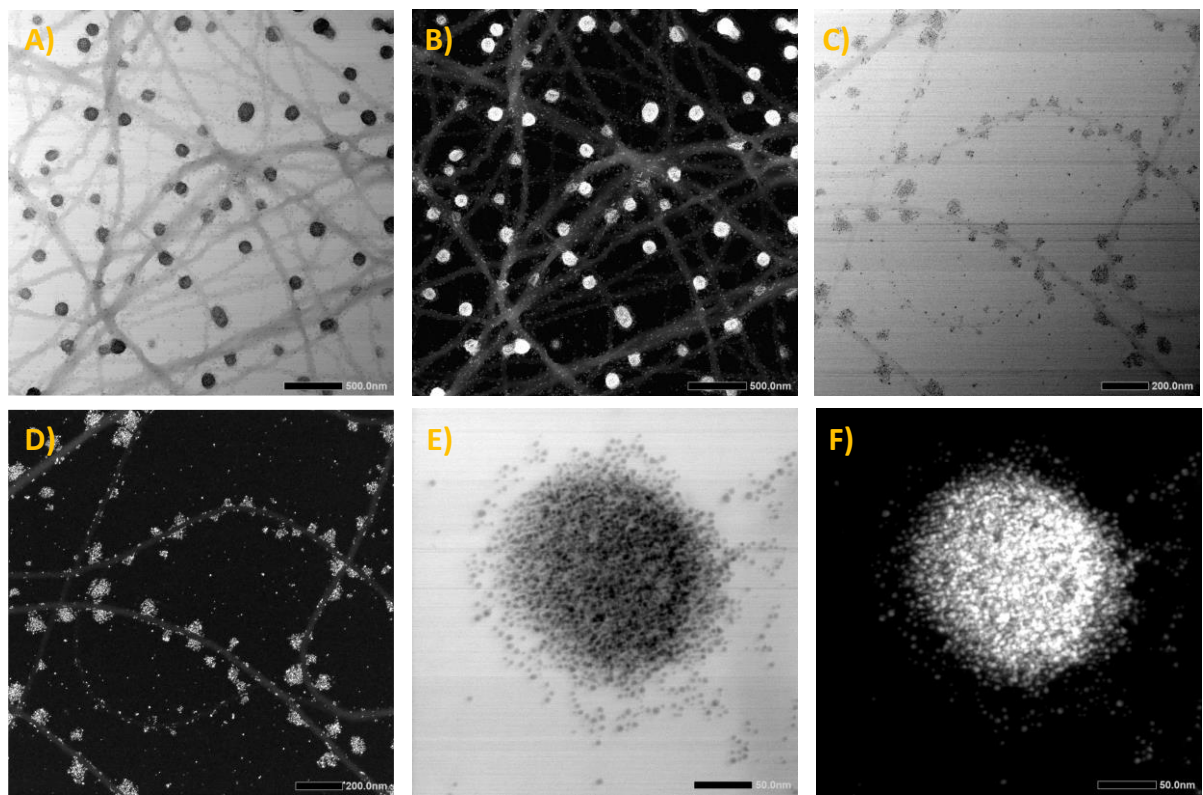


**Fig. S8** Bright field (BF) and dark field (DF) STEM images of different regions of the NCA-1.0 sample.

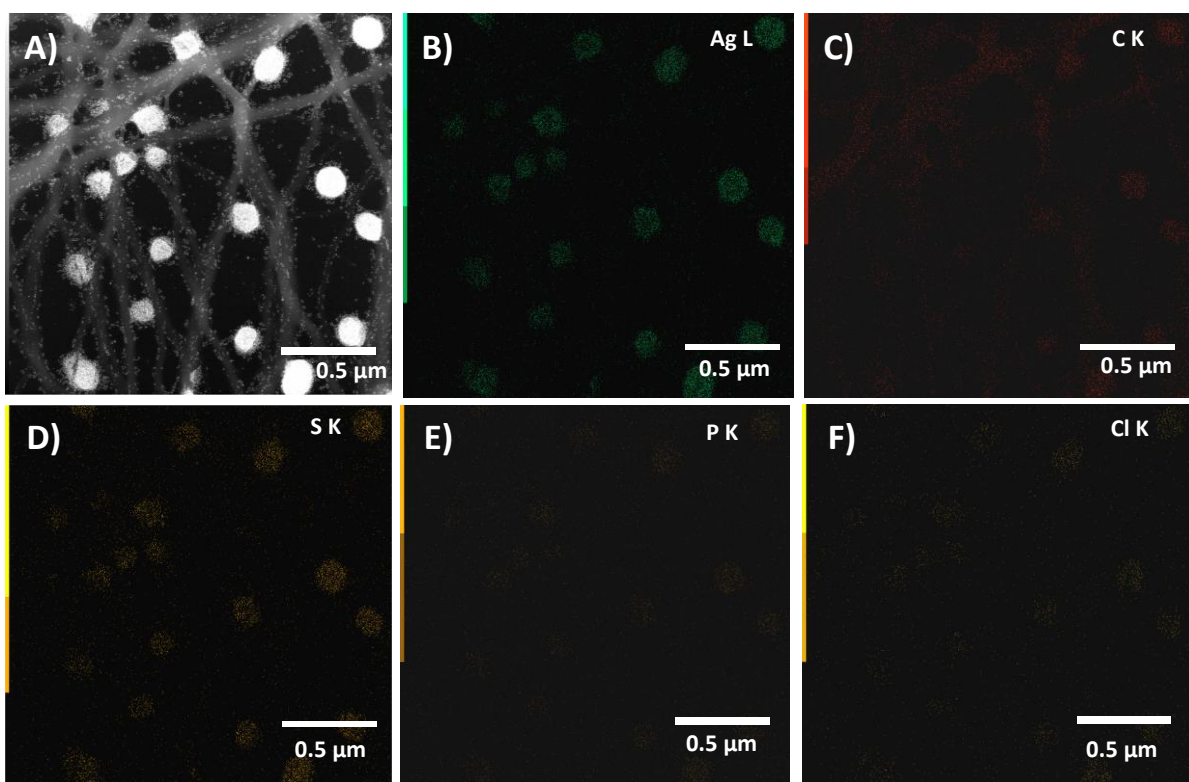


**Fig. S9** STEM-EDS mapping of Ag, C, S, P, and Cl of NCA-1.0.

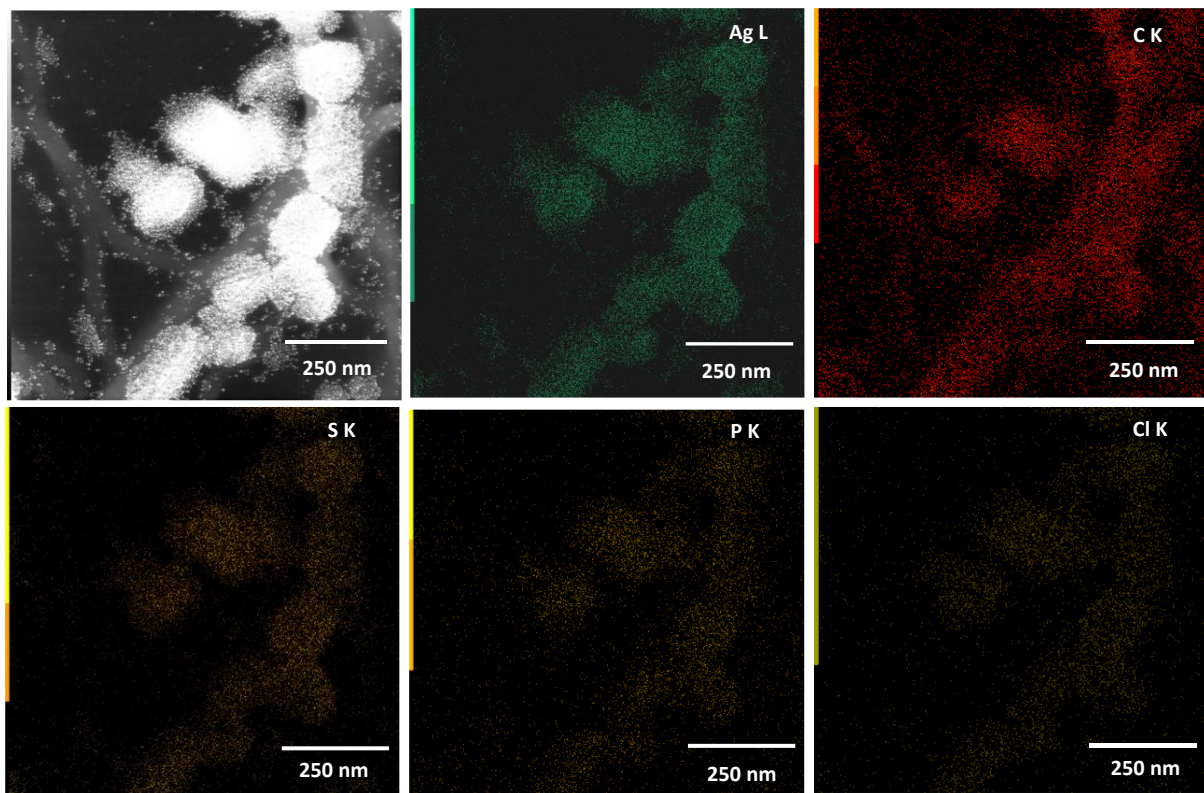


**Fig. S10** STEM-EDS mapping of Ag, C, S, P, and Cl in spherical structures of NCA-1.0.

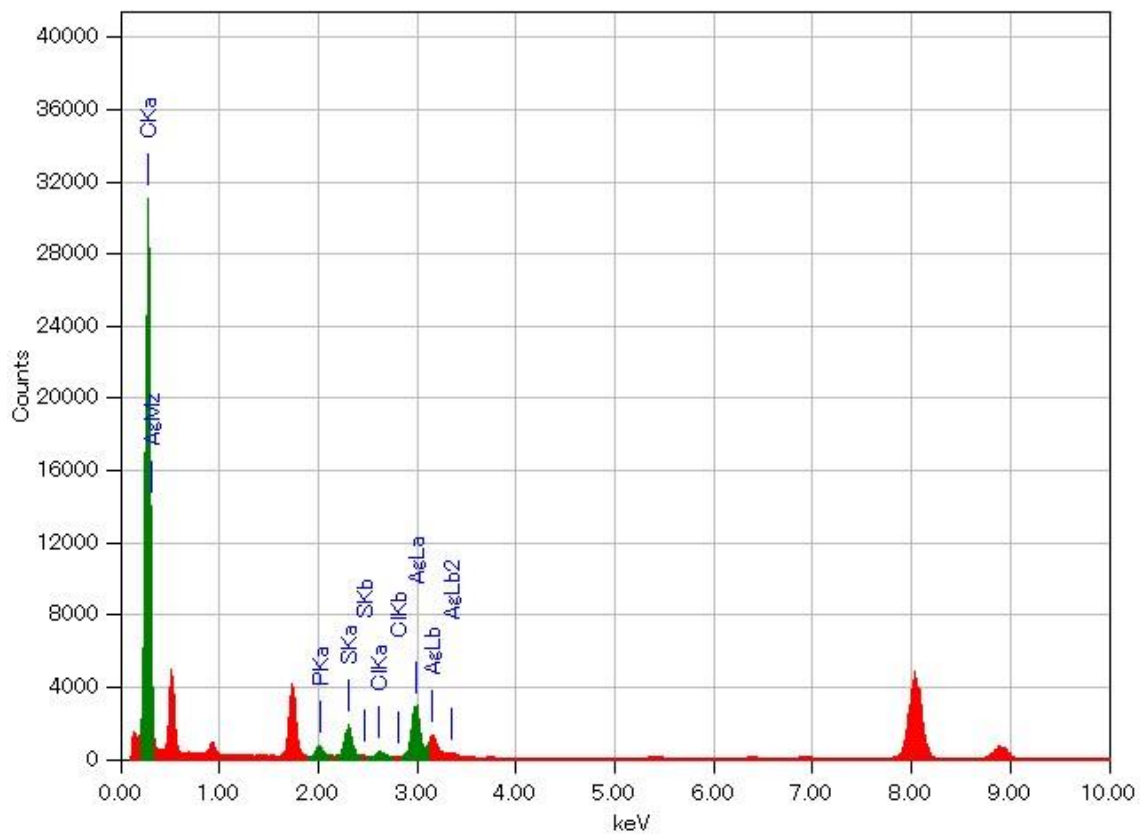


**Fig. S11** EDX spectrum of NCA-1.0.

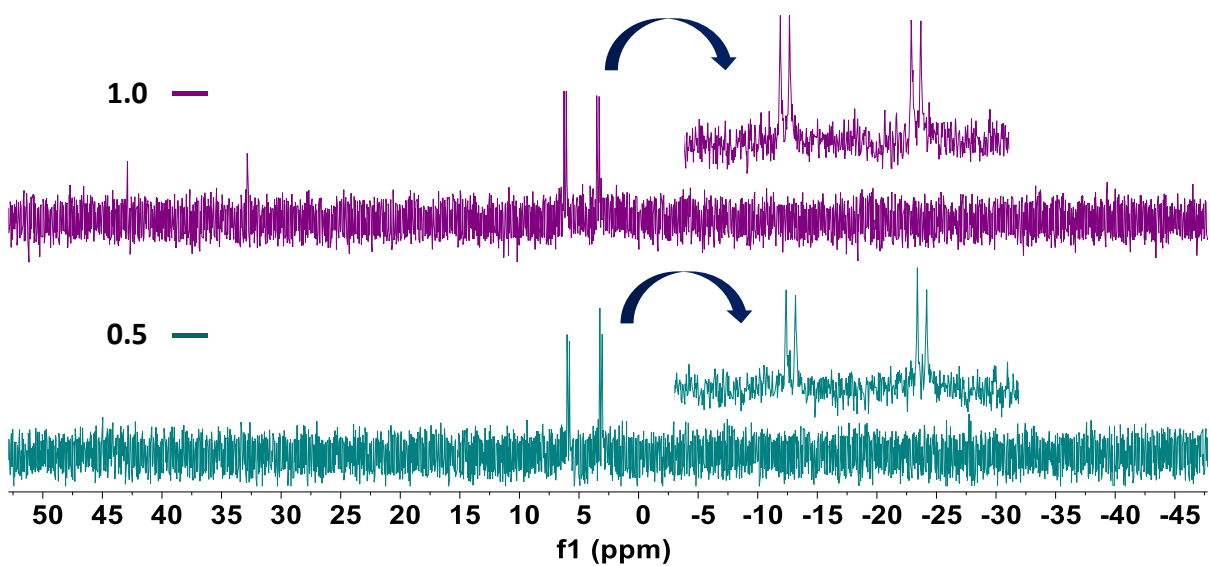


**Fig. S12** The  $^{31}\text{P}$  NMR spectra of NCA 0.5 and NCA 1.0.

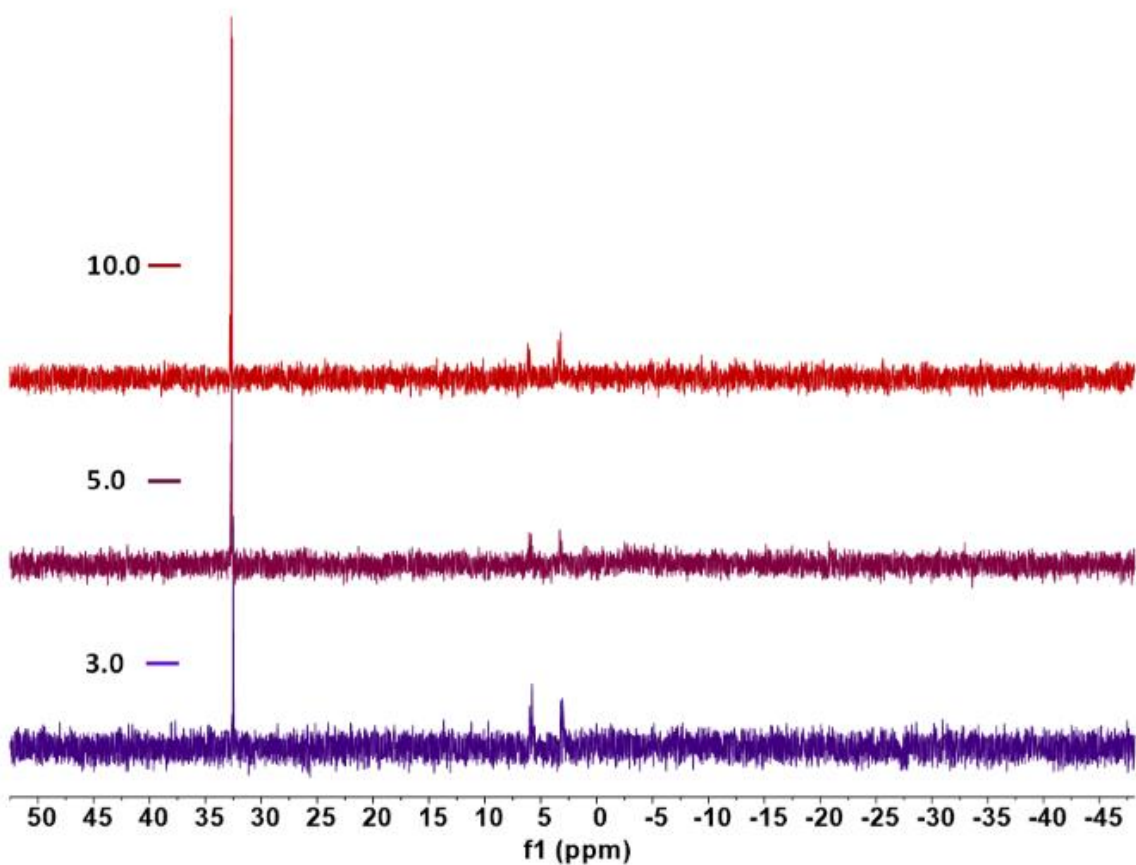


**Fig. S13** The  $^{31}\text{P}$  NMR spectra of NCA 3.0, NCA 5.0, and NCA 10.0.

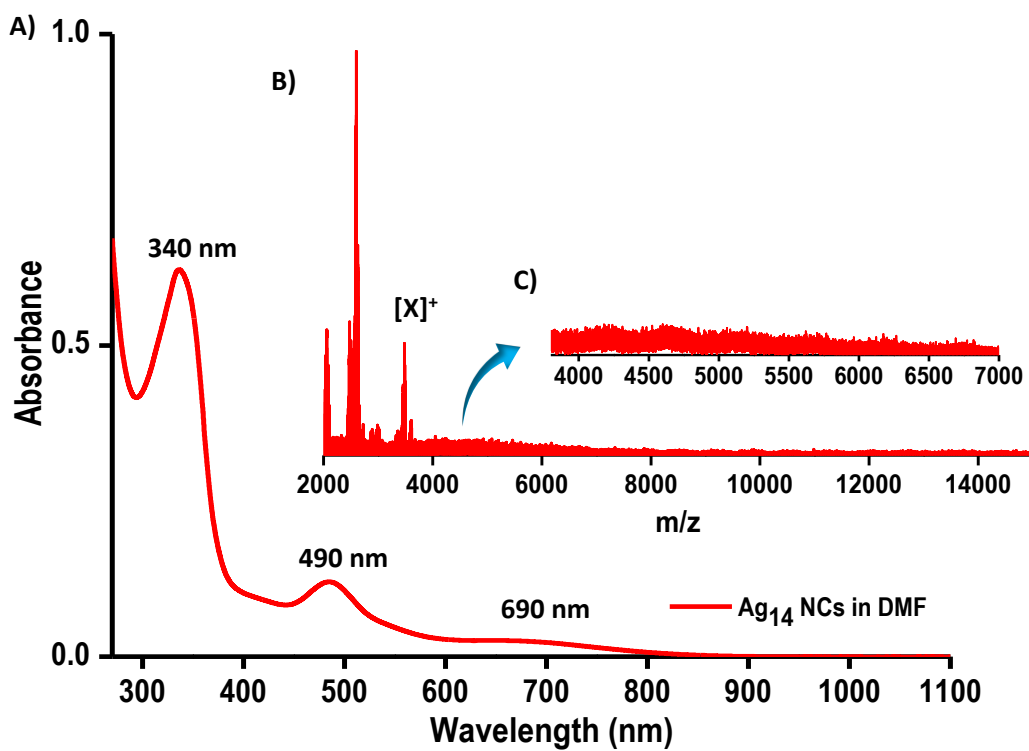


**Fig. S14** A) UV-vis spectrum of NCA-1.0 redispersed in DMF. B) The corresponding ESI MS. C) Enlarged view.

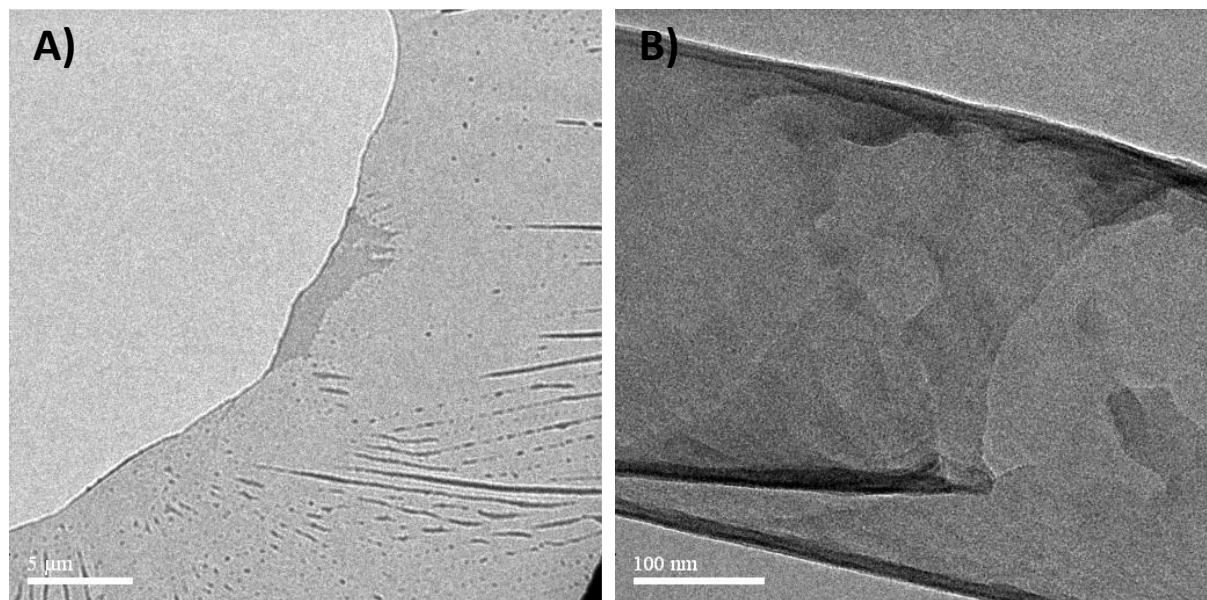


**Fig. S15** A) and B) is the TEM images of the DPPH-NT mixture.

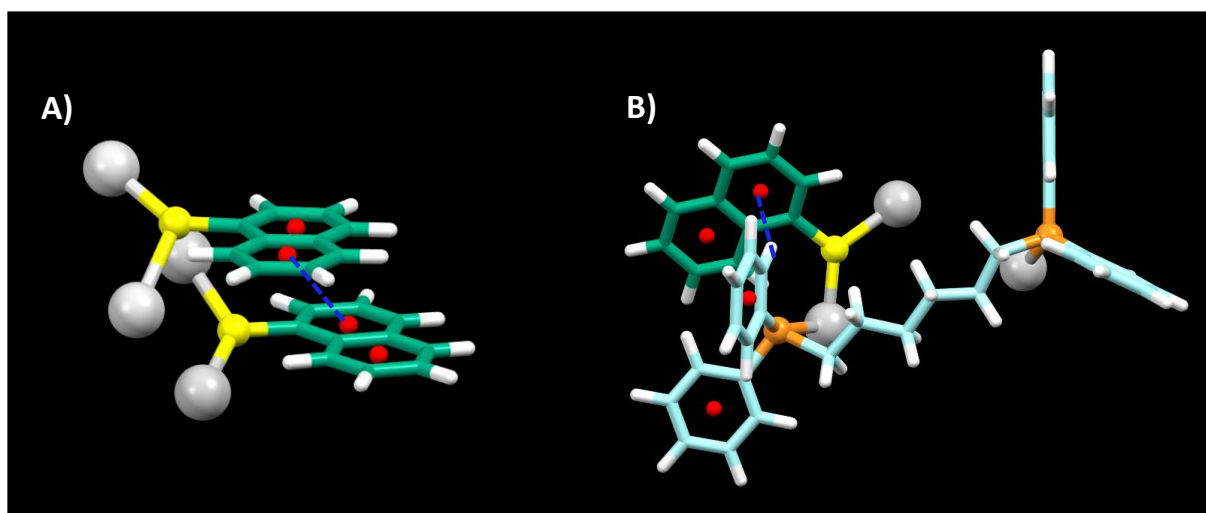


**Fig. S16** Schematic illustration of possible supramolecular interactions in  $\text{Ag}_{14}$  NC assemblies. A)  $\pi \dots \pi$  interactions between NT ligands. B)  $\text{CH} \dots \pi$  interactions between NT and DPPH ligands.

### References

1. D. N. Mastronarde, *Microscopy and Microanalysis*, 2003, **9**, 1182-1183.
2. D. N. Mastronarde, *Journal of Structural Biology*, 2005, **152**, 36-51.
3. N. Nonappa and P. Engelhardt, *Imaging & Microscopy*, 2019, **21**, 22-24.
4. J. R. Kremer, D. N. Mastronarde and J. R. McIntosh, *J Struct Biol*, 1996, **116**, 71-76.
5. P. Engelhardt, in *Encyclopedia of Analytical Chemistry*, DOI: <https://doi.org/10.1002/9780470027318.a1405>.